

# Convolutional discrete Fourier transform method for calculating thermal neutron cross section in liquids

Rong Du<sup>a,b</sup>, Xiao-Xiao Cai<sup>a,b,\*</sup>

<sup>a</sup>*Institute of High Energy Physics, Chinese Academy of Sciences*

<sup>b</sup>*Spallation Neutron Source Science Center*

---

## Abstract

Being exact at both short- and long-time limits, the Gaussian approximation is widely used to calculate neutron incoherent inelastic scattering functions in liquids. However, to overcome a few numerical difficulties, extra physical approximations are often employed to ease the evaluation.

In this work, a new numerical method, called convolutional discrete Fourier transform, is proposed to perform Fourier transform of  $\exp[-f(t)]$ . We have applied this method to compute the differential cross sections of light water up to 10 eV. The obtained results, thoroughly benchmarked against experimental data, showed a much higher dynamic range than conventional fast Fourier transform. The calculated integral cross sections agree closely with the light water data in the state-of-the-art nuclear data library. It is in evidence that this numerical method can be used in the place of the extra physical approximations.

---

## 1. Introduction

The advances of molecular dynamics simulations [1, 2, 3] provided valuable insights into the microscopic structural and dynamic properties of liquids. It has been shown that for the application of thermal neutron scattering, accurate neutron incoherent inelastic scattering in water can be calculated using molecular dynamics simulated

---

\*Corresponding author:

Email address: [caixx@ihep.ac.cn](mailto:caixx@ihep.ac.cn) (Xiao-Xiao Cai)

density of states without any free parameter [4]. Such progress implies that it is now possible to predict the incoherent process reliably prior to any experiment.

However, there exist numerical challenges when evaluating the cross sections numerically using the Gaussian approximation [5], for instance, the highly oscillatory and singular integrand. To tackle the problem, physical approximations are often employed to ease such a computation. Under these approximations, motions of atoms are strictly categorised as a particular type of diffusion and solid-like vibrations. Therefore, available numerical routines, such as the phonon expansion method [6], which are valid for systems that move around equilibrium positions, can be directly used. The final numerical results of the combined models are often consistent with experimental cross sections in many liquids [4].

Apart from that, the main difficulty of the computation lies within the finite numerical dynamic range of Fourier transforms. Discrete Fast Fourier transform is typically used to correlate atomic microscopic structure and dynamics with measurable scattering cross sections, i.e. a function of momentum and energy transfers that can span tens of orders of magnitudes. However, this numerical procedure is known to have spectral leakage [7] from a frequency bin to the others close by. Therefore, a weak and fast decaying signal can be submerged by the leakage from an intense bin, resulting in a significantly smaller dynamic range than the precision that digitised floating-point number can offer. Even when the evaluation of the cross section is assisted with physical approximations, at large energy transfer, e.g. above 1 eV, the numerical error can no longer be ignored. A short-collision-time (STC) approximation is often employed to replace the noise-contaminated results [8].

In this work, we attempt to solve the numerical difficulties using mathematical techniques solely, a convolutional discrete Fourier transform (CDFT) method is proposed as an alternative to the three physical approximations introduced earlier.

In section 2, the theory of neutron scattering and Gaussian approximation, along with the physical approximations for easing numerical calculation, are introduced. The convolutional discrete Fourier transform (CDFT) method is firstly introduced in section 3, and applied to the Gaussian approximation in section 3.1. Using the identical input as the state-of-the-art CAB light water cross section [9, 10], the CDFT calculated

scattering function of light water is benchmarked against differential and integral cross sections in section 4. This work is concluded in section 5.

## 2. Neutron incoherent Inelastic scattering in liquids

### 2.1. Gaussian approximation

In Van Hove's space-time correlations [11], the scattering function  $S(Q, \omega)$  is given by the Fourier transform of the intermediate scattering function  $F(Q, t)$ , which can be approximated by a Gaussian [5]

$$\begin{aligned} S(Q, \omega) &= \frac{1}{2\pi} \int e^{-i\omega t} F(Q, t) dt \\ &= \frac{1}{2\pi} \int e^{-i\omega t} \exp\left[-\frac{Q^2}{2} \Gamma(t)\right] dt \end{aligned} \quad (1)$$

With the fluctuation-dissipation theorem, it has been shown that,  $\Gamma(t)$  in liquids can be expressed as [5]

$$\Gamma(t) = \frac{\hbar}{m} \int_0^\infty d\omega \frac{\rho(\omega)}{\omega} \left[ \coth\left(\frac{\hbar\omega}{2k_B T}\right) (1 - \cos \omega t) - i \sin \omega t \right] \quad (2)$$

Here,  $\rho(\omega)$  is the density of states,  $k_B$  is the Boltzmann constant.

### 2.2. Physical models assisted numerical evaluation

Physical models are often employed to facilitate the evaluation of Eq. 1. This section introduces the conventional formulation for the evaluation briefly, a more detailed discussion can be found in [12]. The key technique for such evaluation is to break down the cumbersome width function  $\Gamma(t)$  into two easier-to-evaluate components, i.e. a diffusion part and a solid-like vibration part.

$$\rho(\omega) = w_d \rho_{\text{diff}}(\omega) + w_v \rho_{\text{vib}}(\omega) \quad (3)$$

Where  $w_d$  and  $w_v$  are the weights satisfy  $w_d + w_v = 1$ . The diffusion component is simply described by the Egelstaff-Schofield model [13]

$$\rho_{\text{diff}}(\epsilon) = \frac{4cw_t}{\pi\hbar kT} \sqrt{c^2 + 1/4} \sinh \frac{\epsilon}{2kT} K_1\left(\frac{\epsilon}{kT} \sqrt{c^2 + 1/4}\right) \quad (4)$$

where  $c$  and  $w_i$  are the diffusion constant and translational weight, respectively.

$$c = \frac{M_{\text{diff}} D}{\hbar} \quad (5)$$

The diffusion coefficient  $D$  that equals  $\pi k T \rho(0)/2m$  is correlated linearly with  $\rho(0)$ , and  $M_{\text{diff}}$  is the diffusion mass.

For the solid-like part, the model that describes neutron-phonon interaction in harmonic crystals are used [6].

$$F(Q, t) = \exp\left[-\frac{Q^2}{2}\gamma(0)\right] \exp\left[\frac{Q^2}{2}\gamma(t)\right] \quad (6)$$

$$= \exp(-2W) \exp\left[\frac{Q^2}{2}\gamma(t)\right] \quad (7)$$

where  $\exp(-2W)$  is the Debye-Waller factor, and

$$\gamma(t) = \frac{\hbar}{m} \int_0^\infty d\omega \frac{\rho_{\text{vib}}(\omega)}{\omega} \left[ \coth\left(\frac{\hbar\omega}{2kT}\right) \cos \omega t + i \sin \omega t \right] \quad (8)$$

Towards zero energy, for any three-dimensional solid material, the density of states always decay according to a power law [14]. Therefore, the integrand of Eq. 8 has no singularity at  $\omega = 0$ . Indicating by Eq. 3, to make this combination of physic approximations work, it is crucial to subtract a suitable portion of the diffusive density of states, i.e.  $\rho_{\text{diff}}$ , from the original liquid state to obtain an  $\rho_{\text{vib}}$  that satisfies the power law at small energies, i.e.  $a\omega^2$ .

At large energy and momentum transfers, the scattering function became a Gaussian without any detailed structures. Due to the numerical difficulties, conventional evaluation is likely to fail in that region, hence the short-collision time approximation is often used.

$$S(Q, \omega) = \sqrt{\frac{1}{4\pi k_b T E_r}} \exp\left[-\frac{(\hbar\omega - E_r)^2}{4\pi E_r}\right], \text{ where } E_r = \frac{\hbar^2 Q^2}{2m} \quad (9)$$

### 3. The convolutional discrete Fourier transform (CDFT) method

The concept of the CDFT method is based on the Taylor expansion of the function for Fourier transform. We discuss the case that the function of interest is an exponential

function  $\exp[-f(t)]$ , and  $f(t) > 0$ . The Fourier transform of that can be expanded as

$$F(\omega) = \int e^{-i\omega t} \exp[-f(t)] dt \quad (10)$$

$$= \sum_{n=0}^{\infty} \frac{1}{n!} \int e^{-i\omega t} [-f(t)]^n dt \quad (11)$$

$$(12)$$

From the Convolution theorem, it is straight forward to have

$$\int e^{-i\omega t} f_1(t) f_2(t) dt = F_1(\omega) \otimes F_2(\omega) \quad (13)$$

Therefore, it is obvious to see that the higher order terms of the summation can be obtained by convoluting the results of lower order terms. However, this method is not numerically stable. The integral area of the convoluted result is the produce of the areas of the two input functions. After a great number of convolutions, the results can exceed the limiting value that can be expressed by a floating number. Therefore, it is desired to use normalised functions as input.

According to Bochner's theorem, the Fourier transform of a probability measure on  $f(t)$  is necessarily a normalized continuous positive-definite function. For a finite discrete function, to make the function continuous in the overall domain of  $t$ , it is required to change the function to make it zero at both boundaries. For an event function, it is obvious to get  $r(t) = f_{max} - f(t)$ . Eq. 10 can then be rearranged as

$$\begin{aligned} F(\omega) &= e^{-f_{max}} \int e^{-i\omega t} e^{r(t)} dt \\ &= e^{-f_{max}} \sum_{n=0}^{\infty} \frac{r^n(0)}{n!} \int e^{-i\omega t} \left[ \frac{r(t)}{r(0)} \right]^n dt \end{aligned} \quad (14)$$

Denoting  $g_n(\omega)$  function as

$$g_n(\omega) = \int e^{-i\omega t} \left[ \frac{r(t)}{r(0)} \right]^n dt \quad (15)$$

It can be see immediately that  $g_0$  is a sinc function and not involved in the convolution procedure. On the other hand, the integral of  $g_1$  is normalised (see Eq. 16) and

is the fundamental input of the convolutions.

$$\begin{aligned}
\int g_1(\omega) d\omega &= \iint e^{-i\omega t} \frac{r(t)}{r(0)} dt d\omega \\
&= \int \delta(t) \frac{r(t)}{r(0)} dt \\
&= 1
\end{aligned} \tag{16}$$

Therefore, the integral of higher order  $g$  functions are also unity.

As  $r(0) = f_{max}$ , Eq. 14 becomes

$$F(\omega) = e^{-f_{max}} \sum_0^{\infty} \frac{(f_{max})^n}{n!} g_n(\omega) \tag{17}$$

Until now, the numerical procedure is straight forward. Here we introduced the distortion factor, which is used to maximise the dynamic range of the convolution.

We defined an distort function as  $e^{a\omega}$ . It has the relation with the convolution as

$$\begin{aligned}
F_1(\omega) \otimes F_2(\omega) &= \int F_1(\mu) \cdot F_2(\omega - \mu) d\mu \\
&= \int e^{a\mu} \hat{F}_1(\mu) \cdot e^{a(\omega - \mu)} \hat{F}_2(\omega - \mu) d\mu \\
&= e^{a\omega} \int \hat{F}_1(\mu) \cdot \hat{F}_2(\omega - \mu) d\mu \\
&= e^{a\omega} \hat{F}_1(\mu) \otimes \hat{F}_2(\omega - \mu)
\end{aligned} \tag{18}$$

Denoting

$$\hat{g}_n(\omega) = e^{-a\omega} g_n(\omega) \tag{19}$$

Using Eq. 18, we finally have,

$$F(\omega) = \exp(-f_{max} + a\omega) \sum_{n=0}^{\infty} \frac{(f_{max})^n}{n!} \hat{g}_n(\omega) \tag{20}$$

where  $a$  is a constant, which only affects the dynamic range of the final convolution. To optimise the result for a higher dynamic range, the CDFT method evaluates the Fourier transform by convoluting the distorted function  $\hat{g}_n(\omega)$ , instead of the original function  $g_n(\omega)$ . The significant improvement of such procedure is introduced in section 4.

### 3.1. Applying the CDFT Method to the cross section calculation

Recall that

$$S(Q, \omega) = \frac{1}{2\pi} \int e^{-i\omega t} \exp\left(-\frac{Q^2}{2} \Gamma(t)\right) dt \tag{21}$$

Using Eq. 14, the integration becomes

$$S(Q, \omega) = \exp\left(-\frac{\Gamma_{max}Q^2}{2}\right) \sum_{n=0}^{\infty} \left(\frac{\Gamma_{max}Q^2}{2}\right)^n \frac{1}{n!} \int e^{-i\omega t} \left[\frac{r(t)}{r(0)}\right]^n dt \quad (22)$$

where  $r(t) = \Gamma_{max} - \Gamma(t)$ . Numerically, this equation is equivalent to the direct fast Fourier transform.

Based on Eq. 20, the integration can also be expressed as

$$S(Q, \omega) = \exp\left(-\frac{\Gamma_{max}Q^2}{2} + a\omega\right) \sum_{n=0}^{\infty} \left(\frac{\Gamma_{max}Q^2}{2}\right)^n \frac{1}{n!} \hat{g}_n(\omega) \quad (23)$$

Note that for our typical calculations are room temperature for light water, we have found that the distortion coefficient  $a = \omega/3k_bT$  works quite well.

At large momentum transfer, the factor  $\exp(\Gamma_{max}Q^2)$  in Eq. 23 may overflow. To prevent that, we apply the convolutional method again. Denoting  $h(\omega) = S(Q, \omega)$ , at a given  $Q$  where the scattering function is obtained by Eq. 23, according to Eq. 21, the scattering function at higher  $Q$  values can be calculated as

$$S(\sqrt{2^{n-1}}Q, \omega) = \underbrace{h(\omega) \otimes h(\omega) \cdots \otimes h(\omega)}_n \quad (24)$$

Notice that the self-scattering function satisfies the sum-rule  $\int S(Q, \omega) d\omega = 1$ , hence a large number of  $h(\omega)$  functions can be convoluted without encountering the numerical overflowing problem. The distortion factor, similar to Eq. 23, are also applied in our numerical implementation.

## 4. Results and discussion

### 4.1. Evaluation of the self-scattering function

The density of states (DOS) for both hydrogen and oxygen in light water for the CAB model are used as the input of our calculation [15]. The data, shown in Fig. 1, are provided by the one of the authors of the CAB model [10].

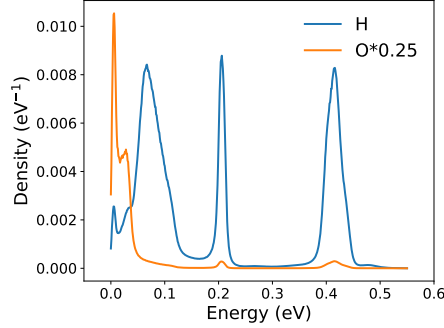


Figure 1: The density of states for hydrogen and oxygen in light water for CAB model at 297 K [15].

The  $\Gamma(t)$  functions defined in Eq. 2 are evaluated using the Filon method [16] in the range between  $-200\text{ps}$  and  $200\text{ps}$ , of which the detailed implementation can be found in Appendix A. For light water, a molecular dynamic simulation of  $100\text{ps}$  is able to capture the important slow dynamics for scattering function [12], the time range chose in this work is considered to be adequate. The result of  $\Gamma(t)$  for hydrogen at 297 K is shown in Fig. 2. Complex fast dynamics are concentrated in the region less than  $1\text{ps}$ . The real part of  $\Gamma(t)$  increases linearly when the physics is mainly governed by the diffusion process at large times.

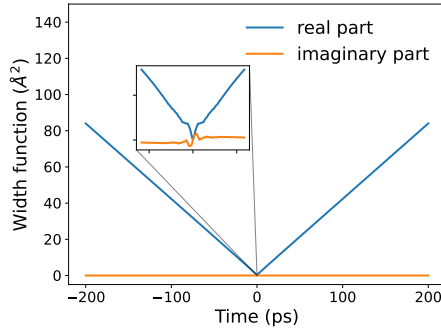


Figure 2: Width function  $\Gamma(t)$  for hydrogen at 297 K.

Fig. 3 compares the numerical results of three different methods for the Fourier transform. The reduced momentum transfer is  $1\text{\AA}^{-1}$ . At small energy transfers, results from three methods are all agreed. When the absolute value of the momentum transfer



is greater than 2eV, the scattering function calculated by the CDFT method showed a much higher dynamic range than the others.

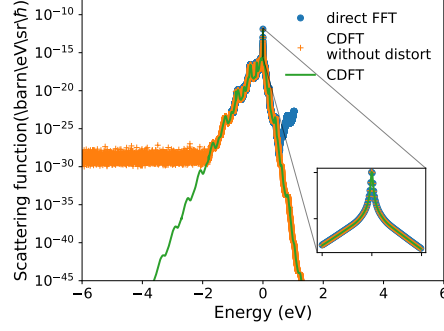


Figure 3: Comparison of calculated scattering function from direct fast Fourier transform (i.e. Eq. 21), CDFT without distortion (i.e. Eq. 22) and with distortion (i.e. Eq. 23),  $Q = 1 \text{ \AA}^{-1}$

When the momentum transfer is very large, the short-collision-time (SCT) approximation becomes valid. Fig. 4 compares the numerical results from direct fast Fourier transform, CDFT method and the prediction of the SCT model, which is only valid when moment transfer is high. The result from the CDFT method showed good agreement with the prediction of SCT method. On the other hand, the results from direct fast Fourier transform agree with neither of the other results, suggesting such a method could suffer from significant error when the momentum transfer is high.

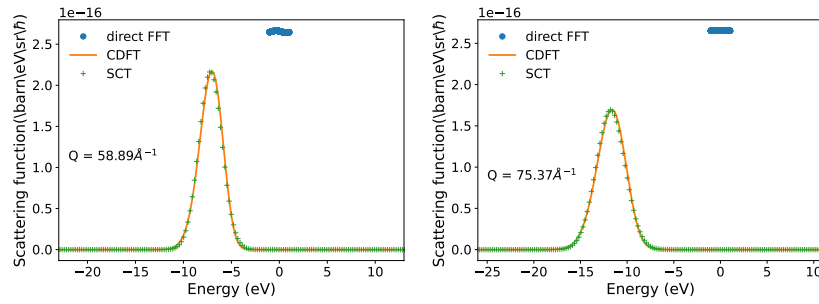


Figure 4: Comparison of calculated scattering function from direct fast Fourier transform (i.e. 21), CDFT with distortion (i.e. Eq. 24) and the prediction of the SCT approximation (i.e. Eq. 9), at larger  $Q$ .

The complete scattering functions for light water molecule is shown in Fig. 5. For

the generation of the data, Eq. 23 and Eq. 24 are used to calculate the function below and above  $Q = 0.3 \text{ \AA}^{-1}$ , respectively. The peak position of the SCT approximation (i.e. Eq. 9) at given  $Q$  are shown as broken lines. These lines are well aligned with the peaked intensities contributed by hydrogen and oxygen.

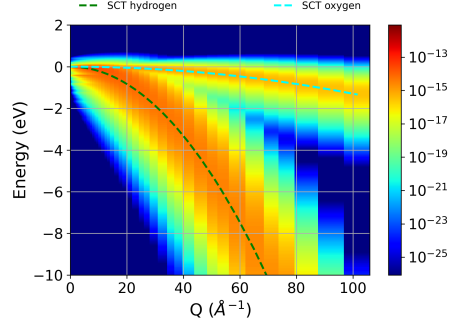


Figure 5: The scattering function of light water at 297 K calculated using Eq. 23 and Eq. 24

#### 4.2. Quasi-elastic scattering

Fig. 6 compares the half width at half maximum (HWHM) of the scattering function at small momentum transfers. Our calculated results are slightly greater than that from a simple isotropic three-dimensional diffusion model (or the Fick's law, see for example chapter 5.4 in [17]). According to that model, the scattering function at small energy and momentum transfers can be described as a Lorentzian

$$S(Q, \omega) = \frac{1}{\pi\hbar} \frac{DQ^2}{(DQ^2)^2 + \omega^2} \quad (25)$$

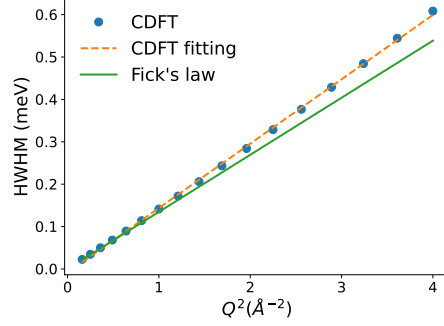


Figure 6: Comparison of the HWHM from CDFT and Fick's law.

The discrepancies are because, unlike the Fick's law, the HWHM from our calculation is not contributed by the diffusive process alone [18]. Fig. 7 shows the contributions to the scattering function from different scattering orders. At small energies, multiple scatterings of diffusive motion and energetic phonons can also contribute to the energy region that the diffusive peak allocated. For example, in a two phonon scattering case, a neutron absorbs and emits phonons of very similar energies. As can be observed in the figure, the contribution from higher order scattering is with a broader HWHM.

The intensity of those peaks grow quickly at greater momentum transfer and the shape diffusion peak will eventually be submerged by the multiple scattering contributions. In that case, the short-collision-time approximation becomes valid.

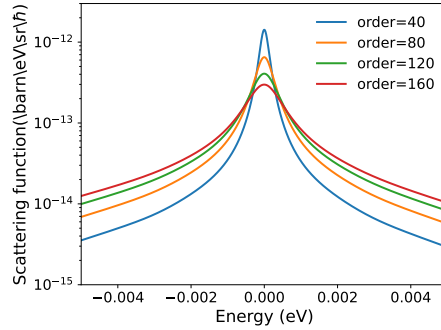


Figure 7: Comparison of scattering function with different scattering orders,  $Q = 1$ .

#### 4.3. Benchmarking against experimental data

The double differential scattering cross section for light water is computed and compared with experiment results from Esch [19]. A comparison for  $E_0 = 0.154$  eV and  $E_0 = 0.632$  eV with different angles were shown in Fig. 8 and Fig. 9. Excellent agreements are observed.

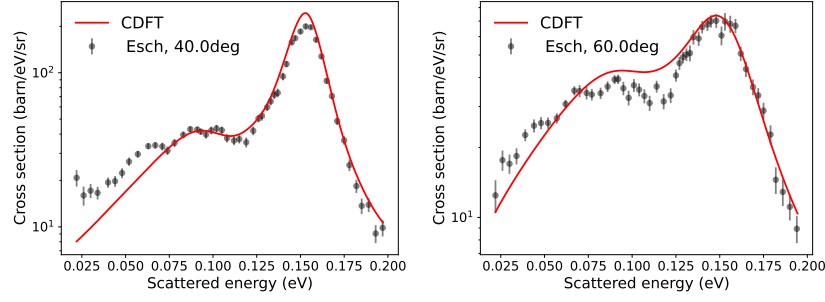


Figure 8: Double differential scattering cross section for light water,  $E_0 = 0.154$  eV.

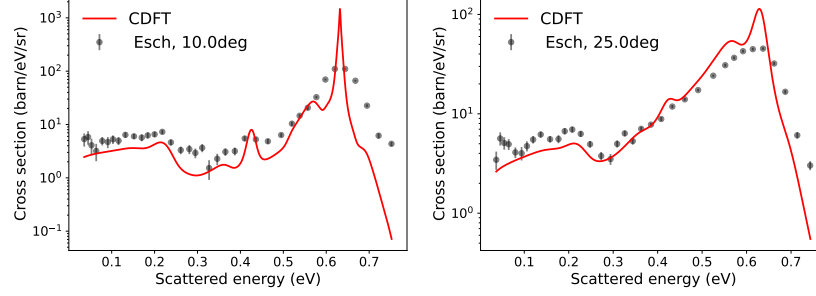


Figure 9: Double differential scattering cross section for light water,  $E_0 = 0.632$  eV .

Total cross section is calculated from  $1 \mu\text{eV}$  to  $10$  eV at  $297$  K to assess the accuracy of the CDFT method. Fig. 10 shows the comparison of several results from both theoretical calculation and experiment, which are from Heinloth (1961) [20] and russell (1966) [21]. Along with the CAB model cross section, the total cross section from the CDFT method are in good agreement with experimental data.

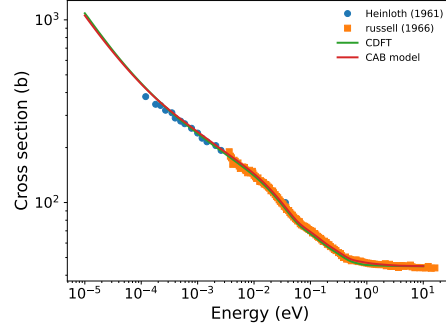


Figure 10: Total cross section for light water at 297 K.

## 5. Conclusion

A numerical procedure, called convolutional discrete Fourier transform (CDFT) method, for evaluating the Fourier transform of an exponential function is proposed. We showed that this method can accurately evaluate neutron incoherent inelastic scattering function in light water. The computed scattering function is consistent with the state-of-the-art CAB model. Instead of physical approximations assisted evaluation of the scattering function, the CDFT method relies on no additional physical approximations. The results from the CDFT method should provide more confidence when working with a new liquid, on with the validity of the commonly used physical approximations are unknown.

The CDFT method will be released in an open source package, along side with the NCrystal project [22].

## Acknowledgements

This research is supported by the National Natural Science Foundation of China (Grant No.12075266). The authors are grateful to Dr. Damian, J. I. Marquez for valuable discussions and substantial support.

## Appendix A. Filon method

The Filon method is used for the integrals of the form:

$$\begin{aligned} S &= \int_a^b f(x) \sin(kx) dx \\ C &= \int_a^b f(x) \cos(kx) dx \end{aligned} \quad (\text{A.1})$$

The equations for numerical implementation are these:

$$S = h[\alpha(f_0 \cos(kx_0) - f_{2p} \cos(kx_{2p})) + \beta S_{2p} + \gamma S_{2p-1}], \quad (\text{A.2})$$

$$C = h[\alpha(f_{2p} \sin(kx_{2p}) - f_0 \sin(kx_0)) + \beta C_{2p} + \gamma C_{2p-1}], \quad (\text{A.3})$$

where

$$S_{2p} = \sum_{i=0}^p f_{2i} \sin(kx_{2i}) - \frac{1}{2}[f_0 \sin(kx_0) + f_{2p} \sin(kx_{2p})], \quad (\text{A.4})$$

$$S_{2p-1} = \sum_{i=1}^p f_{2i-1} \sin(kx_{2i-1}), \quad (\text{A.5})$$

$$C_{2p} = \sum_{i=0}^p f_{2i} \cos(kx_{2i}) - \frac{1}{2}[f_0 \cos(kx_0) + f_{2p} \cos(kx_{2p})], \quad (\text{A.6})$$

$$C_{2p-1} = \sum_{i=1}^p f_{2i-1} \cos(kx_{2i-1}), \quad (\text{A.7})$$

$$\alpha = 1/\theta + \sin(2\theta)/2\theta^2 - (2 \sin^2 \theta)/\theta^3, \quad (\text{A.8})$$

$$\beta = 2[(1 + \cos^2 \theta)/\theta^2 - \sin(2\theta)/\theta^3], \quad (\text{A.9})$$

$$\gamma = 4(\sin \theta/\theta^3 - \cos \theta/\theta^2), \quad (\text{A.10})$$

$$\theta = kh, \quad (\text{A.11})$$

$$f_i = f(x_i), x_{i+1} - x_i = h, x_0 = a, x_{2p} = b \quad (\text{A.12})$$

## References

- [1] F. H. S. Aneesur Rahman, “Molecular dynamics study of liquid water,” *Journal of Chemical Physics*, vol. 55, pp. 3336–3359, 1971.
- [2] K. Toukan, “Molecular-dynamics study of atomic motions in water,” *Physical Review B*, vol. 31, pp. 2643–2648, 1985.
- [3] E. G. J. Martí, J. A. Padro, “Molecular dynamics simulation of liquid water along the coexistence curve: Hydrogen bonds and vibrational spectra,” *Journal of Chemical Physics*, vol. 105, pp. 639–649, 1996.
- [4] G. Noguere, J. P. Scotta, S. Xu, E. Farhi, J. Ollivier, Y. Calzavarra, S. Rols, M. Koza, and J. I. Marquez Damian, “Temperature-dependent dynamic structure factors for liquid water inferred from inelastic neutron scattering measurements,” *Journal of Chemical Physics*, vol. 155, no. 2, p. 024502, 2021.
- [5] A. Rahman, K. S. Singwi, and A. Sjölander, “Theory of slow neutron scattering by liquids. i,” *Physical Review*, vol. 126, pp. 986–996, May 1962.
- [6] A. Sjölander, “Multiphonon processes in slow neutron scattering by crystals,” *Arkiv Fysik*, vol. 14(21), pp. 315–371, 1958.
- [7] F. Harris, “On the use of windows for harmonic analysis with the discrete fourier transform,” *Proceedings of the IEEE*, vol. 66, no. 1, pp. 51–83, 1978.
- [8] R. MacFarlane and A. Kahler, “Methods for Processing ENDF/B-VII with NJOY,” *Nuclear Data Sheets*, vol. 111, pp. 2739–2890, dec 2010.
- [9] J. I. M. Damian, D. C. Malaspina, and J. R. Granada, “Vibrational spectra of light and heavy water with application to neutron cross section calculations,” *Journal of Chemical Physics*, vol. 139, no. 2, p. 024504, 2013.
- [10] J. I. M. Damian. personal communication, Nov 2021.
- [11] L. V. Hove, “Correlations in space and time and born approximation scattering in systems of interacting particles,” *Physical Review*, vol. 95, pp. 249–262, 1954.

- [12] J. M. Damián, J. Granada, and D. Malaspina, “CAB models for water: A new evaluation of the thermal neutron scattering laws for light and heavy water in endf-6 format,” *Annals of Nuclear Energy*, vol. 65, pp. 280–289, 2014.
- [13] P. A. Egelstaff and P. Schofield, “On the evaluation of the thermal neutron scattering law,” *Nuclear Science and Engineering*, vol. 12, no. 2, pp. 260–270, 1962.
- [14] V. F. Sears, E. C. Svensson, and B. M. Powell, “Phonon density of states in vanadium,” *Canadian Journal of Physics*, vol. 73, p. 726, Jan. 1995.
- [15] J. I. M. Damian, D. C. Malaspina, and J. R. Granada, “Vibrational spectra of light and heavy water with application to neutron cross section calculations,” *Journal of Chemical Physics*, vol. 139, p. 024504, 2013.
- [16] L. D. Fosdick, “A special case of the filon quadrature formula,” *Mathematics of Computation*, vol. 22, pp. 77–81, 1968.
- [17] G. L. Squires, *Introduction to the Theory of Thermal Neutron Scattering*. Cambridge University Press, 3 ed., 2012.
- [18] D. Levesque and L. Verlet, “Computer ”experiments” on classical fluids. III. time-dependent self-correlation functions,” *Physical Review A*, vol. 2, pp. 2514–2528, Dec 1970.
- [19] L. J. Esch, M. L. Yeater, W. E. Moore, and K. W. Seemann, “The temperature dependence of neutron inelastic scattering from water,” *Nuclear Science and Engineering*, vol. 46, pp. 223–235, 1971.
- [20] K. Heinloth, “Streuung subthermischer neutronen an h<sub>2</sub>o, ch<sub>2</sub>o<sub>2</sub> und c<sub>6</sub>h<sub>6</sub>,” *Zeitschrift für Physik*, vol. 163, pp. 218–229, 1961.
- [21] H. L. McMurry, G. J. Russell, and R. M. Brugger, “Slow-neutron scattering by water,” *Nuclear Science and Engineering*, vol. 25, pp. 248–260, 1966.
- [22] X.-X. Cai and T. Kittelmann, “Ncrystal: A library for thermal neutron transport,” *Computer Physics Communications*, vol. 246, p. 106851, 2020.



- [23] X.-X. Cai, T. Kittelmann, E. Klinkby, and J. Márquez Damián, “Rejection-based sampling of inelastic neutron scattering,” *Journal of Computational Physics*, vol. 380, pp. 400–407, 2019.